

# Non-equilibrium AC Stark effect and long-lived exciton-polariton states in semiconductor Mie resonators

Andreas Lubatsch<sup>1</sup> and Regine Frank<sup>2,3,4\*</sup>

<sup>1</sup> *Georg-Simon-Ohm University of Applied Sciences, Keßlerplatz 12, 90489 Nürnberg, Germany*

<sup>2</sup> *Institute of Theoretical Physics, Optics and Photonics,*

*Eberhard-Karls University, Auf der Morgenstelle 14, 72076 Tübingen, Germany*

<sup>3</sup> *Bell Laboratories, 600 Mountain Avenue, Murray Hill, NJ 07974-0636 USA*

<sup>4</sup> *Institute of Solid State Physics (TFP), Karlsruhe Institute of Technology (KIT),  
Wolfgang-Gaede Straße 1, 76131 Karlsruhe, Germany*

(Dated: December 19, 2021)

We present Floquet-Keldysh non-equilibrium dynamical mean field calculations (DMFT) with an iterative perturbative solver (IPT) for high pump-power induced Stark states yielding a closing gap within semiconductor bulk and nano-cavities. Our model predicts unusual broadening of bands in systems like ZnO random lasers. This can be explained as an exciton-polariton coupling within the single crystalline pillar meeting the Mie resonance condition. Extraordinary enhancement of the lifetime of electronic states within the gap can lead to stable lasing modes and gain narrowing.

The research of random and polariton lasing has fascinated the community ever since their discovery [1–10]. Both phenomena of coherent emission originating from semiconductor micro-resonators have been interpreted as to be fundamentally different. We show in this letter that on the basis of ultrafast non-equilibrium excitation the groundbreaking implication is possible to interpret random lasing as coupled cavity polariton lasers. On the other hand it would also allow to deduce that semiconductor cavity polariton lasers develop laser thresholds which is the signature of a phase transition.

In this letter we consider the semiconductor bulk as insulator, which is true in the zero temperature limit ( $T = 0$ ), where all lattice influences are frozen out. The gap of 3.3 eV of ZnO corresponds to a Coulomb repulsion  $U$  of about  $U/D = 4.0$ , which is deeply in the Mott insulating regime.  $D$  is the half bandwidth. First, the non-equilibrium bandstructure (i) of a classically strong field pumped bulk ZnO semiconductor is investigated by Keldysh-Floquet non-equilibrium dynamical mean field theory (DMFT) and solved using second order non-equilibrium iterative perturbation theory (IPT). Second we explore topological effects (ii) induced in the non-equilibrium bandstructure when it is coupled to the cavity mode of a geometrical resonator (Fig. 2). By comparison of the life-times of both non-equilibrium solutions we identify long-lived resonances, exciton-polaritons, in the cavity coupled solutions which match in the frequency range experimentally determined spectra of both polariton lasers in ZnO nano-pillars as well as ZnO random lasing experiments.

The Hubbard-type Hamiltonian Eq. (1) describes the electronic dynamics responsible for the generation of microscopic gain and thus leading in further consequence to electronic inversion. It is generalized for electron-photon interaction which is also solved by applying the Floquet-Keldysh formalism using dynamical mean field theory (DMFT) and an iterative perturbative solver (IPT) (see

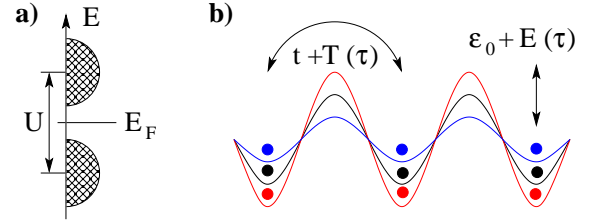


FIG. 1: Insulator to metal transition. (a) Split energy band. The local Coulomb interaction  $U$  determines the width of the gap symmetrical to the Fermi energy  $E_F$ . (b) Electrons in the crystal lattice structure (black). Periodic driving yields an additional hopping contribution  $T(\tau)$  and local renormalization of the lattice energy  $\epsilon_k = \epsilon_0 + E(\tau)$ . The colors represent three time steps of driving.

Fig. 1). The classically field driven cavity-coupled Hamiltonian in position space reads

$$\begin{aligned}
 H = & \sum_{k,\sigma} \epsilon_k c_{k,\sigma}^\dagger c_{k,\sigma} + \frac{U}{2} \sum_{i,\sigma} c_{i,\sigma}^\dagger c_{i,\sigma} c_{i,-\sigma}^\dagger c_{i,-\sigma} \\
 & - t \sum_{\langle ij \rangle, \sigma} c_{i,\sigma}^\dagger c_{j,\sigma} \\
 & + i \vec{d} \cdot \vec{E}_0 \cos(\Omega_L \tau) \sum_{\langle ij \rangle} (c_{i,\sigma}^\dagger c_{j,\sigma} - c_{j,\sigma}^\dagger c_{i,\sigma}) \\
 & + \hbar \omega_o a^\dagger a + g \sum_{k,\sigma} c_{k,\sigma}^\dagger c_{k,\sigma} (a^\dagger + a).
 \end{aligned} \quad (1)$$

The first term  $\sum_{k,\sigma} \epsilon_k c_{k,\sigma}^\dagger c_{k,\sigma}$  denotes the onsite processes which is completed by  $\frac{U}{2} \sum_{i,\sigma} c_{i,\sigma}^\dagger c_{i,\sigma} c_{i,-\sigma}^\dagger c_{i,-\sigma}$  devoted to the Coulomb interaction  $U$  between electrons with opposite spins. The third term  $-t \sum_{\langle ij \rangle, \sigma} c_{i,\sigma}^\dagger c_{j,\sigma}$  denotes the hopping processes with the amplitude  $t$  between nearest neighbored sites. The last three terms are devoted to photons, including the external field-

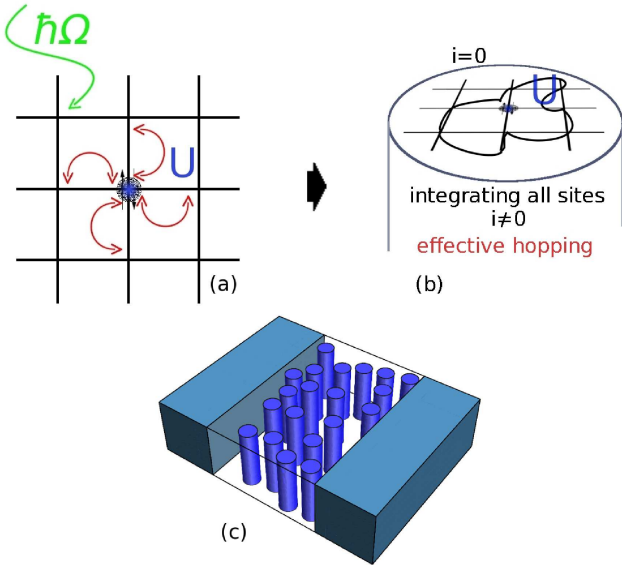


FIG. 2: (a) The semiconductor behaves in this regime as an insulator: In the non-equilibrium DMFT-scheme optical excitation yields electronic hopping processes. They are mapped to the interaction with the single site on the background of the surrounding lattice (bath). (b) Integration over all sites leads to an effective theory including non-equilibrium excitation. This approach here is self-consistent because the bath consists of these very same single sites. The driven electronic system is additionally coupled to a cavity-resonance, the Mie resonance. (c) Experimentally relevant setup, a disordered waveguide of ZnO nanostructures embedded in a Si wafer.

electron coupling, the kinetic energy of the cavity photons and the cavity photon-electron interaction. In  $i\vec{d} \cdot \vec{E}_0 \cos(\Omega_L \tau) \sum_{\langle ij \rangle} (c_{i,\sigma}^\dagger c_{j,\sigma} - c_{j,\sigma}^\dagger c_{i,\sigma})$  is noted the renormalization of the hopping processes due to classical interaction of the dipole moment  $\vec{d}$  with an external time dependent electric field of the amplitude  $\vec{E}_0$ , the pumping laser.  $\tau$  denotes its time dependency and  $\Omega_L$  the corresponding laser frequency. The last two terms denote the cavity mode  $\hbar\omega_0 a^\dagger a$  at the resonance frequency  $\omega_0$  as well as the coupling of this resonance to the electronic density of states  $g \sum_{k,\sigma} c_{k,\sigma}^\dagger c_{k,\sigma} (a^\dagger + a)$  with coupling strength  $g$ . The creator (annihilator) of a cavity photon is denoted  $a (a^\dagger)$  and of an electron it is  $c (c^\dagger)$ . The subscript  $k$  denotes the site,  $i, j$  denote next neighbored sites (Fig. 1) within the originally assumed single-band. The first four terms of Hamiltonian Eq. (1) describe (i) externally pumped bulk semiconductor.

The explicit time dependence of the external field yields Green's functions that depend on two separate time arguments. A double Fourier transform from time- to frequency space leads to relative and center-of-mass frequency [13, 14]

$$G_{mn}^{\alpha\beta}(\omega) = \int d\tau_1^\alpha d\tau_2^\beta e^{-i\Omega_L(m\tau_1^\alpha - n\tau_2^\beta)} e^{i\omega(\tau_1^\alpha - \tau_2^\beta)} G(\tau_1^\alpha, \tau_2^\beta)$$

$$\equiv G^{\alpha\beta}(\omega - m\Omega_L, \omega - n\Omega_L). \quad (2)$$

$(m, n)$  label the Floquet modes and  $(\alpha, \beta)$  address the branch of the Keldysh contour ( $\pm$ ) where the respective time argument resides. Floquet modes describe the Fourier-transformation of a periodic potential in time as the principal structure of bands in frequency space. However the physical consequence which is noteworthy is a quantized absorption and emission of energy quanta  $\hbar\Omega_L$  of and to the original classical field. For non-interacting electrons the analytical solution for  $G_{mn}(k, \omega)$  is solving the equation of motion. Photo-induced hopping leads to the retarded Green's function for this sub-system

$$G_{mn}^R(k, \omega) = \sum_\rho \frac{J_{\rho-m}(A_0 \tilde{\epsilon}_k) J_{\rho-n}(A_0 \tilde{\epsilon}_k)}{\omega - \rho\Omega_L - \epsilon_k + i0^+}, \quad (3)$$

where  $\tilde{\epsilon}_k$  represents the dispersion relation induced by the external field and is to be distinguished from  $\epsilon$  the lattice dispersion. The  $J_n$  are the cylindrical Bessel functions of integer order,  $A_0 = \vec{d} \cdot \vec{E}_0$  and  $\Omega_L$  is the laser frequency. The physical Green's function is given according to

$$G_{\text{Lb}}^R(k, \omega) = \sum_{m,n} G_{mn}^R(k, \omega). \quad (4)$$

The Hamiltonian is solved through single-site Floquet-Keldysh DMFT (IPT) [12, 15]. This requires strict periodicity of the lattice and homogeneous driving. That condition implies Bloch states and is characterized by the wave vector  $k$  within the laser-band-electron Green's function  $G_{\text{Lb}}^R(k, \omega)$ . Due to these requirements and the additional cavity in our system the DMFT selfconsistency relation, the centerpiece of DMFT, assumes the form of a matrix equation of dimension  $2 \times 2$  in Keldysh space of the nonequilibrium Green's functions and of dimension  $n \times n$  in Floquet space. As DMFT solver we generalized the iterated perturbation theory (IPT) to Keldysh-Floquet form as well. The resulting numerics, although challenging, proves to be efficient and stable also for all values of the Coulomb interaction  $U$ . Whereas we consider in [15] a renormalized lattice potential, we take into account here a coupling of the microscopic dipole moment to the external field amplitude [13, 14]. This implies the quantum-mechanical character of the dipole operator  $\hat{d} = i\vec{d} \sum_{\langle ij \rangle} (c_{i,\sigma}^\dagger c_{j,\sigma} - c_{j,\sigma}^\dagger c_{i,\sigma})$  in the fourth term of Eq.(1). It is fundamentally different from the generic kinetic hopping of the third term. The coupling  $\hat{d} \cdot \vec{E}_0 \cos(\Omega_L \tau)$  under the assumption of the Coulomb gauge  $\vec{E}(\tau) = -\frac{\partial}{\partial \tau} \vec{A}(\tau)$ , which reads in Fourier space  $\vec{E}(\Omega_L) = i\Omega_L \cdot \vec{A}(\Omega_L)$ , generates the factor  $\Omega_L$  that cancels the  $1/\Omega_L$  term in the renormalized cylindrical Bessel function in Eq. (7) of ref. [15]. Consequently we consider the first  $n = 10$  Floquet modes only which has been proven to be sufficient here.

The physical consequences are fascinating since in the non-equilibrium externally pumped state the con-

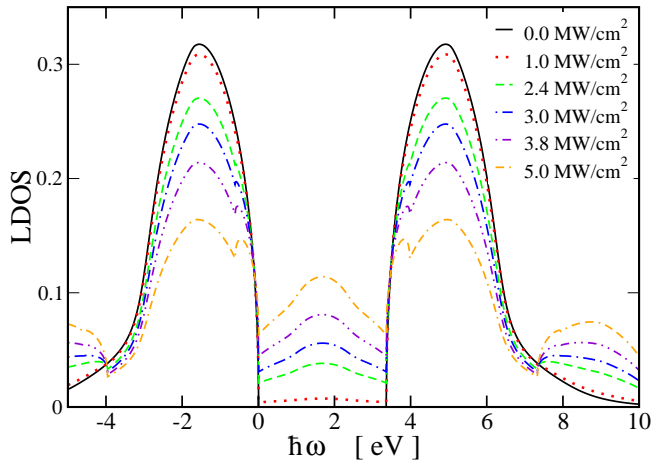


FIG. 3: LDOS for ZnO bulk semiconductor. In equilibrium the electronic gap is  $3.38\text{eV}$ , the microscopic dipole moment equals  $|d| = 2.30826288 \times 10^{-28}\text{Cm}$ , the lattice constant  $a = 0,325\text{nm}$ . The pump power is increased from 0 to  $5.0\text{MW}/\text{cm}^2$ . A significant shift of states into the semiconductor gap is observed. This energy region has been experimentally identified to be the gain area for polaritonic states. Corresponding life times can be found in Fig. 4.

ventional bulk semiconductor ZnO exhibits a counter-intuitive behavior. The parameters are chosen such that the resulting band split equals the ZnO semiconductor band gap of  $3.3\text{eV}$  in the non-pumped case. Through classical external excitation a multi-band insulator develops, where the quantized exchange manifests itself in a multitude of sub-bands. The original bandgap of  $3.3\text{eV}$  is subsequently occupied with dressed states or excitons [16]. The complex permittivity is defined as  $\hat{\epsilon} = \epsilon [1 - i\frac{\sigma}{\omega\epsilon}] = \epsilon' - i\epsilon''$  where  $\epsilon' = \epsilon_r\epsilon_0$  is the real part of the permittivity. The optical conductivity determines the imaginary part  $\omega\epsilon'' = \sigma/\omega\epsilon$

$$\sigma(\Omega_L, i\omega) = \sum_m \frac{8e^2t^2}{2\pi^3} \int d\epsilon N_0(\epsilon) \times \int d\omega' (\text{Im } G_{0m}^R(\epsilon, \omega', \Omega_L))^2 \frac{\partial}{\partial \omega'} F_{0m}^{neq}(\omega', \Omega_L), \quad (5)$$

and characterizes the microscopic gain spectrum (see refs.[11, 15]).

The optical cavity and the Fano-coupling [17] to the electronic subsystem of the bulk semiconductor is described (ii) in the last term of the original Hamiltonian, Eq.(1). It yields an additional contribution to the self-energy  $\Sigma$  in the denominator of the retarded Green's function Eq.(3). The form of  $\Sigma$  significantly triggers the numerical efficiency of the selfconsistency consideration. The strength  $g$  of the coupling between optically excited electrons  $c_{k,\sigma}^\dagger c_{k,\sigma}$  and the cavity resonance  $\hbar\omega_0 a^\dagger a$  has to be considered  $g < 1$  in order to guarantee convergence of the perturbation series up to second or higher order.

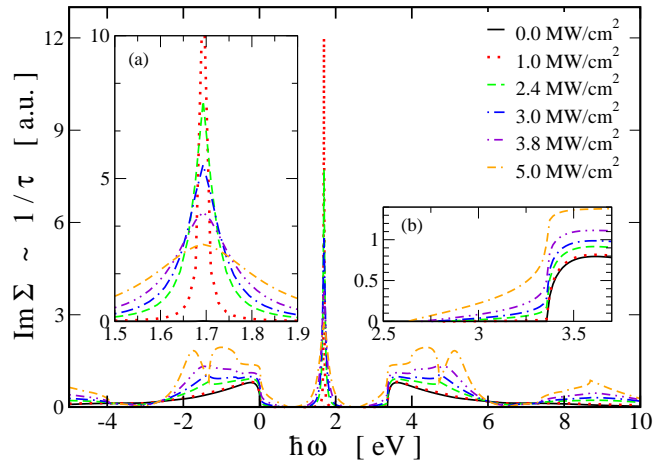


FIG. 4: Inverse lifetime  $1/\tau$  corresponding to the LDOS (Fig. 3) for increasing pump power. (a) The peak centered at  $1.69\text{eV}$  indicates small lifetimes, fast decay of mid-gap states (red emission). (b) Finite lifetime of non-equilibrium states near the band edge indicate stable states which can couple to geometric (Mie) resonances and form cavity-polaritons. With rising pump power the lifetime drops but remains larger than the lifetime of nearby excitonic states in the band.

Our results for the non-equilibrium bandstructure (i) of the classically excited ZnO bulk (Fig. 3) show for increasing pump strengths (colored graphs) spectral weight inside the semiconductor band gap whereas for zero excitation (black curve) the original semi-circular bandstructure for non-interacting systems (band-width assumed to be  $1.7\text{eV}$ ) splits through the Coulomb interaction  $U$  in upper and lower band. The tails at the outer upper and lower bandedges are typical for results derived by the DMFT (IPT) solver. It is found that the additional Floquet bands emerge with increasing pump intensity. Further the development of moderate sub gaps towards the near-gap band edges at  $-0.67\text{eV}$  and  $4.05\text{eV}$  (compared to the bandedge of the valence band) is seen whereas the band edges themselves show a sharp step towards the novel spectral weight inside the gap. Interestingly the relation of the sub-gaps and the simultaneously found features in the results for the non-equilibrium lifetimes  $1/\text{Im}\Sigma$  of the excited states (see Fig. 4) is non-trivial. We find for the same excitation wavelength ( $\lambda = 710\text{nm}$ ) and a raising intensity the increase of the non-equilibrium lifetime at the Fermi edge (see Fig. 4a). Also  $1/\tau$  is larger in the gap near the band edges which corresponds with a higher local density of electronic states (LDOS), i.e. a rising mobility. A plateauing of lifetimes is observed near the edge, whereas deep in the band at  $4.8\text{eV}$  we derive for increasing intensity a crossover. Here  $1/\tau$  develops a peak towards  $|E_0^2| = 3.8\text{MW}/\text{cm}^2$  which flips into a sharp dipped feature (red dash-dots) and arrives at a lifetime almost as high as in the non-excited case (black

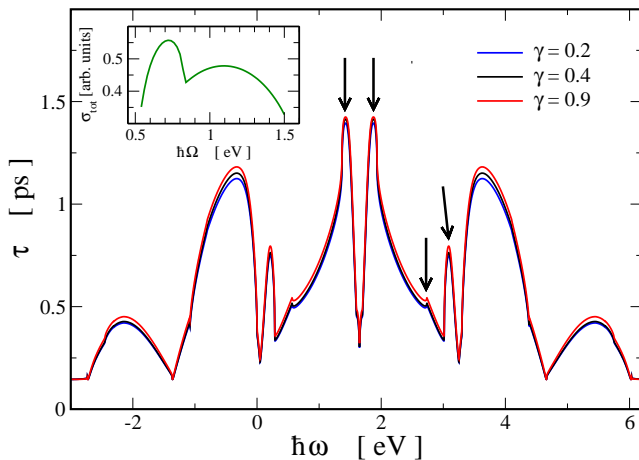


FIG. 5: Polaritonic lifetimes. Pump frequency  $\lambda = 710 \text{ nm}$ , cavities resonance  $\lambda = 505.34 \text{ nm}$ , refractive index  $n = 1.97182$ , pump intensity  $2.4 \text{ MW/cm}^{-2}$ . The difference to pure bulk material is evident in novel, sharp features (marked) at  $0.0.5 \text{ eV}$  and  $2.5..3.3 \text{ eV}$ . These energies correspond to spectrally separated lasing peaks in random laser systems [18]. Tuning the coupling strength of bulk matter and cavity yields small effects. *Inset*: Optical DC-conductivity of the semiconductor Mie resonator for  $\gamma = 0.2$  representing  $|\chi|^3$  processes.

line). This behavior is rather unexpected however it is confirmed by a consistency check of the Floquet sum.

As results for the cavities (Fig. 5) we derive profound changes compared to pure bulk which are only in parts expected. The nano-pillar shall support a single whispering gallery mode.  $a^\dagger$  ( $a$ ) creates (annihilates) a photon as the energy eigen-state at  $\hbar\omega_0 = 2,45 \text{ eV}$  ( $\equiv 505.34 \text{ nm}$ ). This is the *in-plane* Mie resonance, which is related to the continuum of dressed electronic states (Fig. 4) and so the non-equilibrium complex refractive index of ZnO. The momentum of the cavity photon is small compared to the electron's momentum and  $q_{\text{photon}} \simeq 0$  is set whenever we consider the electronic subsystem. We compare the lifetime for varying coupling strength ( $g/t$ ) = 0.2, 0.4, 0.9 at zero temperature and at half filling, yielding a suppression of the spectral function around the Fermi-level (half width of the gap) where electrons are transferred to the high (low) energy tails of the spectral function. Our results are derived for a pumping intensity of  $2.4 \text{ MW/cm}^2$  which is typical for solid state random lasers. In agreement with results for the bulk we also find the characteristic feature around the Fermi edge. Also the dip at  $4.8 \text{ eV}$  persists in the cavity system. The physical interpretation of the non-equilibrium lifetimes including the Mie resonance in (Fig. 4) leads to ultrafast electro-optical Kerr effects, non-equilibrium  $|\chi|^3$  processes with are of the order of  $0.75 \text{ ps}$  up to  $1.25 \text{ ps}$ . This is a long-living cavity polariton which couples to the non-equilibrium AC Stark effect of the pure excited bulk. The peaks in the lifetime of the semiconductor cavity around  $2.8 \text{ eV}$  and  $3.2 \text{ eV}$  are occurring comparably far from the cavi-

ties resonance frequency and so they are a proof of the importance of the Fano resonance for electronic spectrum in general and they express the splitting in several relevant polariton branches which define the lasing frequencies. This is a property of the independent single scatterer, which as for the random lasing experiments, only profits from randomness by the increased impinging photonic intensity. The optical DC-conductivity (inset Fig.4) of the semiconductor Mie resonator for  $\gamma = 0.2$  in the non-equilibrium, i.e.  $|\chi|^3$  processes in the non-equilibrium, shows a strong frequency-dependency and remarkable features which have not been reported before to the best of our knowledge. The dips may lead to significant gain narrowing.

Our results suggest, that solid state random lasers can be interpreted as coupled cavity polariton lasers where the Mie cavity plays a crucial role in the generation of topological features in the microscopic electronic bandstructure of the semiconductor. We theoretically demonstrated polaritonic gain in ZnO as non-equilibrium effect in the Hubbard Model. The polaritonic states are comprised of long-lived excitonic AC Stark states in the original ZnO gap and the Mie resonances of ZnO nano-pillars. This implies that the ZnO laser plasma is actually a polariton condensate which may display a threshold behavior. To distinguish between the concept of either cavity polaritons or excitons and the particle hole plasma and additionally the influence of the mode, i.e. the quality and the coupling of the cavity, a temperature dependent DMFT in the the non-equilibrium will be useful. This novel theoretical approach leads to a more fundamental understanding of ultrafast topological effects in semiconductor nano-cavities.

**Acknowledgments.** RF thanks P. Guyot-Sionnest for highly efficient discussions within the conference TIDS15 *Transport in Interacting Disordered Systems*.

---

\* Correspondence should be addressed to: r.frank@uni-tuebingen.de

- [1] Y. Yamamoto, Nature **405** 629-630 (2000).
- [2] H. Deng, G. Weihs, C. Santori, J. Bloch, Y. Yamamoto, Science, **298** 199-202 (2002).
- [3] H. Cao et al., Phys. Rev. A **55**, 4632 (1997).
- [4] A. Imamoglu, R. J. Ram, S. Pau, Y. Yamamoto, Phys. Rev. A **53**, 4250-4253 (1996).
- [5] J. Kasprzak et al., Nature **443**, 409-414 (2006).
- [6] C. Schneider et al., Nature **497**, 348-352 (2013).
- [7] F. Li et al., Appl. Phys. Lett. **102**, 191118 (2013).
- [8] T. Guillet et al., Appl. Phys. Lett. **99**, 161104 (2011).
- [9] D. Bajoni, J. Phys. D: Appl. Phys. **45** 313001 (2012).
- [10] S. Koghee, M. Wouters, Phys. Rev. Lett. **112**, 036406 (2014).
- [11] A. Georges, G. Kotliar, W. Krauth, M. J. Rozenberg, Rev. Mod. Phys. **68** (1), 13 (1996).

- [12] A. Lubatsch, J. Kroha, Ann. Phys. (Berlin) **18**, No. 12, 863–867 (2009).
- [13] R. Frank, Phys. Rev. B **85**, 195463 (2012),
- [14] R. Frank, Ann. Phys. (Berlin) **525**, No. 1-2, 66-73 (2013).
- [15] R. Frank, New J. Phys. **15** 123030 (2013).
- [16] D. A. B. Miller *et al.*, Phys. Rev. Lett. **53** 22, 2173-2176 (1984), D. S. Chemla *et al.*, Journal of Luminescence **44** 233-246 (1989).
- [17] U. Fano, Phys. Rev. **A** 124, 1866 (1961).
- [18] A. Lubatsch, R. Frank, New J. Phys. **16**, 083043 (2014).